ORGANOMETALLICS

pubs.acs.org/Organometallics Article

H_2 Activation across Manganese(I)−C Bonds: Atypical Metal−Ligand Cooperativity in the Aromatization/Dearomatization Paradigm

Vipulan Vigneswaran, Preshit C. Abhyankar, Samantha N. MacMillan, and David C. Lacy*

Cite This: *Organometallics* 2022, 41, 67−75 Read Online

ACCESS | Metrics & More | Article Recommendations | Supporting Information

ABSTRACT: Dehydrohalogenation of *fac*-Mn(κ^2-*N,P*-PicP)$(CO)_3$Br ($\mathbf{1^H}$) and *fac*-Mn(κ^2-*N,P*-LutP)$(CO)_3$Br ($\mathbf{1^{Me}}$) with equimolar K[N($SiMe_3$)$_2$] afforded the reactive, aromatized 18-electron complexes *fac*-Mn(κ^3-*N,C,P*-PicP)$(CO)_3$ ($\mathbf{2^H}$) and *fac*-Mn(κ^3-*N,C,P*-LutP)$(CO)_3$ ($\mathbf{2^{Me}}$), respectively, with atypical binding modes. $\mathbf{2^H}$ and $\mathbf{2^{Me}}$ activate H_2 across the Mn(I)−C bond to furnish hydride complexes *fac*-Mn(κ^2-*N,P*-PicP)$(CO)_3$H ($\mathbf{4^H}$) and *fac*-Mn(κ^2-*N,P*-LutP)$(CO)_3$H ($\mathbf{4^{Me}}$), respectively. Both $\mathbf{2^H}$ and $\mathbf{2^{Me}}$ were observed to produce dearomatized 18-electron complexes Mn(κ^2-*N,P*-PicP*)$(CO)_4$ ($\mathbf{3^H}$) and Mn(κ^2-*N,P*-LutP*)$(CO)_4$ ($\mathbf{3^{Me}}$), respectively, when reacted with CO. The reactive Mn(I)−C moiety of $\mathbf{2^H}$ and $\mathbf{2^{Me}}$ reacts with a variety of electrophiles: benzyl cyanide to form *fac*-Mn(κ^3-*N,N′,P*-(LutP-BnCN))$(CO)_3$ (**6**), *E*-chalcone to form *fac*-Mn(κ^3-*N,C,P*-LutP-chalcone)$(CO)_3$ (**7**), and $AlCl_3$ to form *fac*-Mn(κ^3-*N,Cl,P*-PicP-$AlCl_3$)$(CO)_3$ ($\mathbf{8^H}$) and *fac*-Mn(κ^3-*N,Cl,P*-LutP-$AlCl_3$)$(CO)_3$ ($\mathbf{8^{Me}}$) featuring a rare intramolecular Mn-(μ-Cl)-Al moiety. Mn(I)-catalyzed Michael addition was explored. Dehydrohalogenation of $\mathbf{1^H}$ with alkoxides afforded the substituted complex *fac*-Mn(κ^2-*N,P*-PicP)(OR)$(CO)_3$ ($\mathbf{10^H}$) that was also reactive toward H_2 forming $\mathbf{4^H}$. Under identical conditions with alkoxide bases, $\mathbf{1^{Me}}$ affords $\mathbf{2^{Me}}$ demonstrating dichotomous behavior. We also explored the *i*Pr-substituted analogues of $\mathbf{1^H}$ and $\mathbf{1^{Me}}$ ($\mathbf{11^H}$ and $\mathbf{11^{Me}}$, respectively) and found them to be essentially identical in behavior. Complexes $\mathbf{1^R}$ and $\mathbf{11^R}$ were found to be excellent catalysts for styrene hydrogenation. The relevance of the κ^3-*N,C,P* binding mode discovered herein to catalysis is briefly discussed.

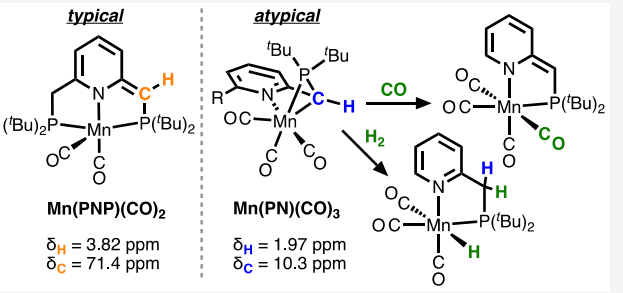

INTRODUCTION

Manganese(I)−carbonyl complexes are potential alternatives to traditional second- and third-row homogeneous catalysts for a myriad of different transformations such as ruthenium(II)-catalyzed (de)hydrogenation and dehydrogenative coupling of organic substrates.[1] The ability of Mn(I) with bifunctional ligands to replicate chemistry that uses similarly coordinated Ru(II) systems implicates parallel modes of metal−ligand cooperativity (MLC).[2,3] At least two major paradigms in MLC have emerged: Noyori-type α metal−ligand cooperativity (α-MLC)[4] and aromatization/dearomatization-type MLC (A/D-MLC).[5] Typically, inroads into these modes are achieved through formal dehydrohalogenation of a precatalyst to generate an unsaturated 16-electron complex. These in turn activate H_2 to generate an 18-electron metal hydride across M−L bonds via MLC steps. In α-MLC, dehydrohalogenation generates an unsaturated 16-electron complex featuring an amido moiety, whereas in A/D-MLC, dehydrohalogenation generates an unsaturated 16-electron complex featuring a dearomatized pyridine/amido moiety (Scheme 1). It is noteworthy that in both of these paradigms there is no formal change in the oxidation state of the metal, a key characteristic of MLC.

In a previous report from our group, we studied Mn(I)-aminophosphine systems and their use in transfer hydro-

Scheme 1. α versus A/D MLC in Bidentate Mn(I) Systems

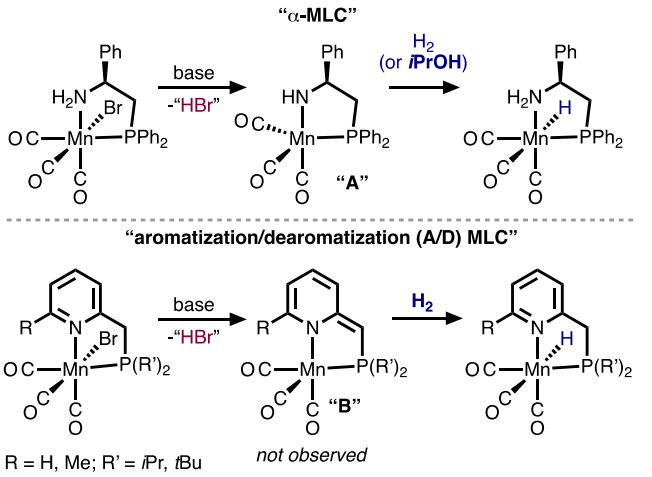

Received: October 22, 2021
Published: December 29, 2021

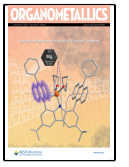

https://doi.org/10.1021/acs.organomet.1c00606
Organometallics 2022, 41, 67−75

genation of ketones and chalcones (Scheme 1, top).[6] In a head-to-head comparison, we observed that the amino-phosphine-based system was capable of ketone transfer hydrogenation, but a 2-picolinylphosphine complex was inactive. Because the nominally active Mn(I)−H species can be generated either through α-MLC (in "**A**") or via A/D-MLC (in "**B**"), we were intrigued by the disparity in outcomes, especially given that the picoline-based system was recently shown to be competent toward alkene hydrogenation and is reproduced herein.[7]

Hence, we endeavored to explore the coordination chemistry of the 2-picolinyl di-*tert*-butylphosphine (PicP$^{t\mathrm{Bu}}$) ligand from our previous report and its lutidinyl analogue (LutP$^{t\mathrm{Bu}}$). Notably, the dehydrohalogenation of the Mn(I) precatalysts afforded a novel isomeric form of the expected dearomatized complex **B**, the κ^3-*N,C,P* complex $\mathbf{2}^{\mathbf{R}}$ (Scheme 2). Importantly, this novel coordination mode is not

Scheme 2. Atypical MLC Studied in This Work

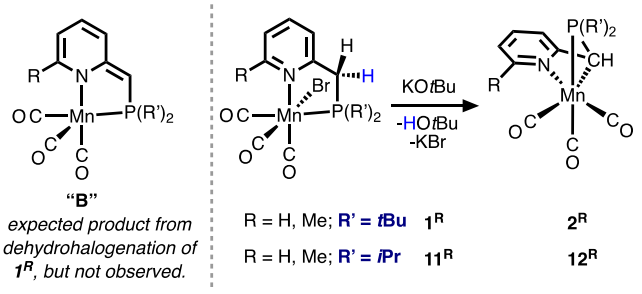

deleterious to catalysis, as these compounds catalyze Michael additions and alkene hydrogenation. The reactivity of the isomeric form featuring the κ^3-*N,C,P* coordination mode with a Mn(I)−C bond suggests that pyridine-based systems may, at times, operate through α-MLC rather than A/D-MLC. This revelation offers new possibilities for catalytic intermediates to consider in mechanistic investigations, especially during catalyst activation. The role of ligand steric bulk was also explored in detail.

RESULTS AND DISCUSSION

Preparation of κ^3-*N,C,P*-Mn(I) Complexes with K[N(SiMe$_3$)$_2$]. Treatment of the ligands PicP and LutP with equimolar Mn(CO)$_5$Br in refluxing petroleum ether (1.5 h) afforded the yellow-orange coordination complexes Mn(PicP$^{t\mathrm{Bu}}$)(CO)$_3$Br ($\mathbf{1}^{\mathbf{H}}$) and Mn(LutP$^{t\mathrm{Bu}}$)(CO)$_3$Br ($\mathbf{1}^{\mathbf{Me}}$), respectively, in high yields; when referred to mutually, the differently substituted complexes will be designated with an "R" superscript (e.g., $\mathbf{1}^{\mathbf{R}}$). The ^{31}P{^{1}H} chemical shifts of $\mathbf{1}^{\mathbf{H}}$ and $\mathbf{1}^{\mathbf{Me}}$ are 88 and 84 in $CDCl_3$, respectively. The three carbonyl ligands are facially coordinating as indicated by Fourier transform infrared (FTIR) spectroscopy and confirmed by X-ray diffraction (XRD) (Figure 1); as mentioned, $\mathbf{1}^{\mathbf{H}}$ was previously reported by us.[6] We also prepared the *i*Pr$_2$P analogues [e.g., Mn(PicP$^{i\mathrm{Pr}}$)(CO)$_3$Br is $\mathbf{11}^{\mathbf{H}}$,[7] and Mn(LutP$^{i\mathrm{Pr}}$)(CO)$_3$Br is $\mathbf{11}^{\mathbf{Me}}$] that will be discussed below.

Activation of precatalysts such as $\mathbf{1}^{\mathbf{R}}$ is most commonly achieved using an alkoxide base like KO*t*Bu or NaO*t*Bu, but the chemistry of $\mathbf{1}^{\mathbf{R}}$ with alkoxides resulted in complicated mixtures and is discussed below (*vide infra*). In contrast, the reactions with K[N(SiMe$_3$)$_2$] furnished a single product and are discussed first (Scheme 3). Treatment of $\mathbf{1}^{\mathbf{R}}$ with 1 equiv of

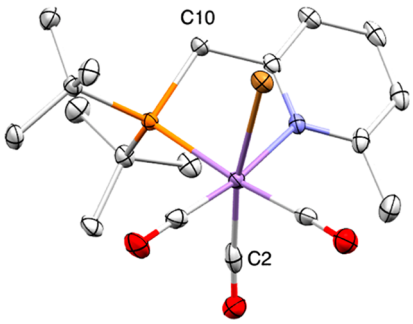

Figure 1. X-ray crystallographically determined molecular structure of $\mathbf{1}^{\mathbf{Me}}$ with thermal ellipsoids set at 50% probability. Hydrogen atoms have been omitted for the sake of clarity. The structure of $\mathbf{1}^{\mathbf{H}}$ is described elsewhere.[6] Color scheme (used throughout): Mn, purple; nitrogen, blue; oxygen, red; carbon, gray; phosphorus, orange; bromine, brown; chlorine, lime green; boron, pink; aluminum, pastel pink. Selected bond distances (angstroms) and angles (degrees) for $\mathbf{1}^{\mathbf{Me}}$: Mn−N, 2.152(2); Mn···C10, 3.138(3); Mn−P, 2.3649(6); C2−Mn−Br, 168.23(9).

Scheme 3. Preparation of κ^3-*N,C,P*-Mn(I) Complexes

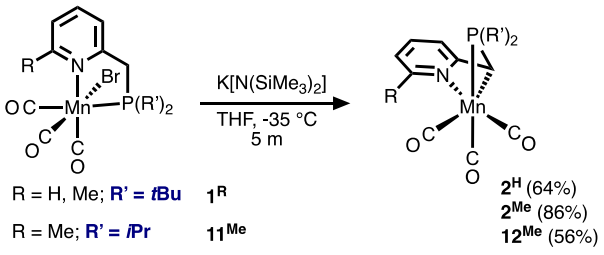

K[N(SiMe$_3$)$_2$] in dry tetrahydrofuran (THF) at −35 °C afforded $\mathbf{2}^{\mathbf{R}}$, whose *fac*-κ^3-*N,C,P* scorpionate coordination mode was confirmed through XRD (Figure 2). The bond lengths of the pyridine ring are fully consistent with an aromatized mode, and the Mn−C$_{methine}$ distance is 2.2 Å, significantly shortened compared to that of the unbound compounds in this report (e.g., ∼3.1 Å). $\mathbf{2}^{\mathbf{R}}$ is structurally isomeric to their expected dearomatized counterparts (i.e., $\mathbf{2}^{\mathbf{R}*}$), albeit we have not observed these unsaturated 16-electron complexes and note that such coordination is effectively unknown for bidentate Mn(I) systems.

The *fac*-κ^3-*N,C,P* coordination mode persists in solution as determined using two-dimensional nuclear magnetic resonance (NMR) spectroscopy in C_6D_6. The benzylic−C*H* ^{1}H NMR resonances for $\mathbf{2}^{\mathbf{H}}$ and $\mathbf{2}^{\mathbf{Me}}$ appear at δ_H 2.00 and 2.06, respectively, and these are correlated (*g*HSQC) with ^{13}C NMR resonances at δ_C 10.0 and 9.6, respectively. ^{31}P{^{1}H} NMR reveals single peaks at δ_P 115 and 113 for $\mathbf{2}^{\mathbf{H}}$ and $\mathbf{2}^{\mathbf{Me}}$, respectively. The upfield ^{1}H and ^{13}C resonances are consistent with the formal Mn−CH moiety of the *fac*-κ^3-*N,C,P* coordination mode rather than the dearomatized mode. For instance, the known dearomatized Mn(PNP$^{t\mathrm{Bu}}$)(CO)$_2$ complex shows an olefinic carbon (i.e., the site of deprotonation) at δ_C 71.4 correlating to δ_H 3.82 (Chart 1).[8] Similar *fac*-κ^3-*L,C,P* coordination modes have been observed for Mn,[9] but not in systems that can dearomatize.

Thermal Stability of κ^3-*N,C,P* Mn(I) Complexes. Investigation of the thermal stability revealed dichotomous chemical behavior between $\mathbf{2}^{\mathbf{H}}$ and $\mathbf{2}^{\mathbf{Me}}$. When an NMR sample of $\mathbf{2}^{\mathbf{H}}$ in C_6D_6 was heated gradually from room temperature to 70 °C over 4 days, ^{1}H and ^{31}P{^{1}H} NMR peaks characteristic

https://doi.org/10.1021/acs.organomet.1c00606
Organometallics 2022, 41, 67−75

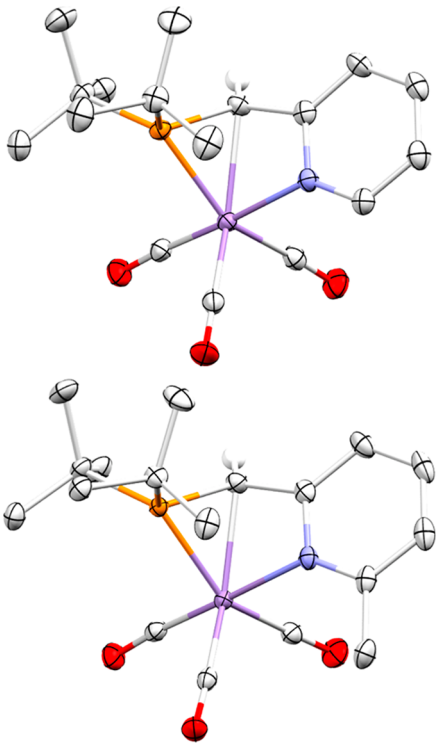

Figure 2. X-ray crystallographically determined molecular structures of 2^{H} (top) and 2^{Me} (bottom) with thermal ellipsoids set at 50% probability. Hydrogen atoms have been omitted for the sake of clarity except for the methylene CH proton. Selected bond distances (angstroms) for 2^{H}: Mn−N, 2.054(1); Mn−$C_{methine}$, 2.205(2); Mn−P, 2.2663(6). Selected bond distances (angstroms) for 2^{Me}: Mn−N, 2.079(1); Mn−$C_{methine}$, 2.206(1); Mn−P, 2.2545(5).

Chart 1. ^{1}H and ^{13}C NMR Features for 2^{H} and Mn(PNP^{tBu})(CO)$_2$ in Toluene-d_8[8]

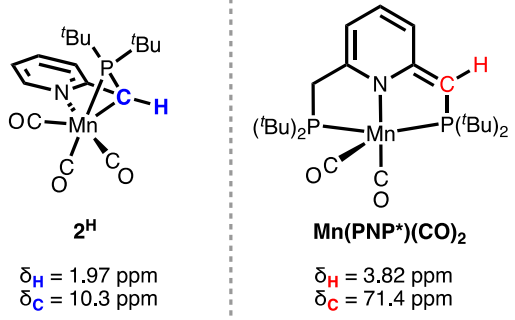

of 2^{H} were observed to gradually disappear while new signals consistent with a structure having a dearomatized ligand (3^{H}) appeared (Figures S24 and S25). Specifically, the Mn−C*H* resonance at δ_H 2.00 gradually disappeared and was replaced with a new resonance at δ_H 3.36 and was correlated to a ^{13}C NMR signal at δ_C 61.64, characteristic of a deprotonated and dearomatized benzylic position. Congruently, the sharp peak at δ_P 115 for 2^{H} in the ^{31}P{^{1}H} NMR spectrum slowly disappeared with the gradual appearance of a very broad apparent multiplet centered at δ_P 98. Both spectroscopic changes are accompanied by a change in color from orange to dark red; the dark red color is anecdotally characteristic of dearomatization of the pyridine ring. In summary, these observations suggested that 3^{H} contains a dearomatized ligand.

Drop-cast FTIR-ATR of the NMR solution contained several CO stretches, and we hypothesized that the major component 3^{H} was a tetracarbonyl complex (Figure S26). To account for the extra carbonyl ligand in 3^{H}, decomposition must have occurred; indeed, free ligand and a fine black precipitate accompany the formation of 3^{H} under these conditions, and the transformation is not reversible. In contrast to chemistry associated with conversion of 2^{H} to 3^{H}, no changes to 2^{Me} were observed under identical conditions.

To bolster our tetracarbonyl hypothesis for 3^{H}, we treated 2^{H} with CO (10% in argon), resulting in quantitative formation of 3^{H} without any decomposition (Scheme 4 and

Scheme 4. Synthetic Routes to 3^{H}

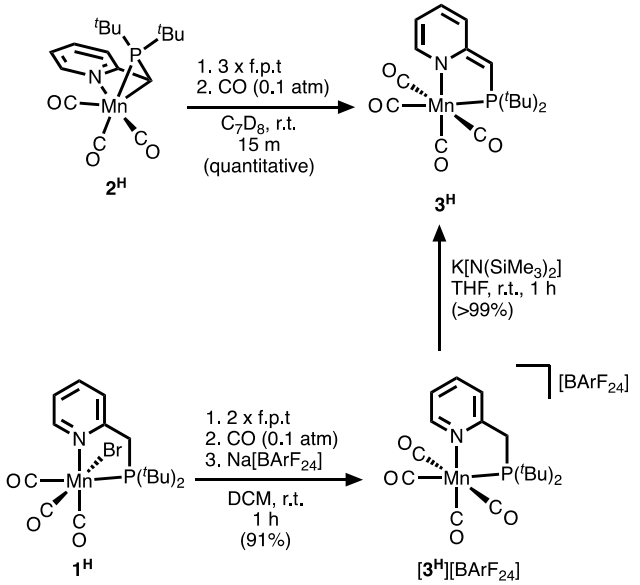

Figures S14−S18). Attempts to isolate and characterize 3^{H} in the solid state were unsuccessful, leading to only decomposition products. Under similar conditions, 3^{Me} can be formed from 2^{Me}. However, only approximately 50% conversion was observed after 4 days at room temperature (Figures S32 and S33).

We also synthesized the cationic aromatized tetracarbonyl complex [3^{H}][$BArF_{24}$] by treating 1^{H} with Na[$BArF_{24}$] in CH_2Cl_2 under a 10% CO atmosphere (Scheme 4). Complex [3^{H}][$BArF_{24}$] was observed to have a broadened ^{31}P{^{1}H} NMR signal at δ_P 100, similar to that of 3^{H}. XRD confirmed our spectroscopic charaterization of [3^{H}][$BArF_{24}$] as a cationic, tetracarbonyl complex featuring an aromatized ligand (Figure 3). Deprotonation of [3^{H}][$BArF_{24}$] by K[N(SiMe$_3$)$_2$] in THF affords 3^{H} (Scheme 4 and Figures S19 and S20).

The broad ^{31}P NMR signals associated with 3^{H} and [3^{H}][$BArF_{24}$] indicate dynamic CO ligand exchange. This was confirmed by performing a variable -temperature NMR study of 3^{H} under CO (10% in argon) in which the broadened peak coalesces at low temperature to a single sharp feature at δ_P 97 (Figures S21 and S23).

When 2^{H} was treated with equimolar PPh_3, the dearomatized complex [{PicP′}Mn(*fac*-CO)$_3$$PPh_3$] ($3^{H/PPh_3}$) was formed. Complex $3^{H/PPh_3}$ features a methylene ^{1}H NMR signal at δ_H 3.84 with a relative integration of one proton, indicative of a dearomatized complex (Figure S34). This signal is correlated to a ^{13}C signal at δ_C 66.5, analogous to 3^{H} (Figure

https://doi.org/10.1021/acs.organomet.1c00606
Organometallics 2022, 41, 67−75

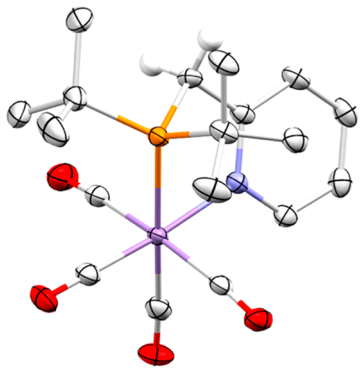

Figure 3. X-ray crystallographically determined molecular structure of $[3^{H}][BArF_{24}]$ with thermal ellipsoids set at 50% probability. Hydrogen atoms have been omitted for the sake of clarity except for the methylene CH proton. The counterion is not shown. Selected bond distances (angstroms): Mn−N, 2.088(1); Mn···$C_{methylene}$, 3.150(1); Mn−P, 2.3663(8).

S37). $^{31}P\{^{1}H\}$ NMR shows two doublets at δ_P 110.8 and 59.4 with a $^{2}J_{PP}$ of 32 Hz, suggesting that the two phosphines are in a *cis* conformation with respect to each other and hence a facial tricarbonyl motif (Figure S35). Solutions of complex $3^{H/PPh_3}$ in C_6D_6 show conversion to 3^{H} over time, accompanied by release of a free ligand and PPh_3 (Figure 4). Altogether, these results point to a labile dearomatized system.

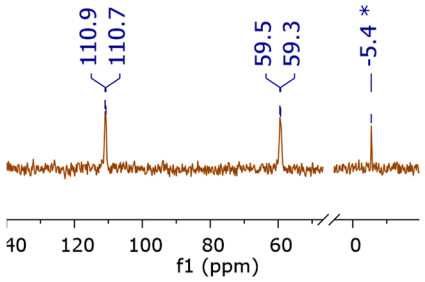

Figure 4. $^{31}P\{^{1}H\}$ NMR spectrum of $3^{H/PPh_3}$ in C_6D_6. The asterisk denotes PPh_3.

Computational Assessment of κ^3-*N,C,P* Stability, Ligand Effects, and Isomerization. We propose the following mechanistic scheme to account for the various observations surrounding the chemistry of 2^{R} and 3^{R}. The first product of dehydrohalogenation is the *fac*-κ^3-*N,C,P* coordination mode as found in 2^{R} and is the thermodynamically favored isomer in all cases ($PicP^{R}$ and $LutP^{R}$, where R = *t*Bu or *i*Pr) over its dearomatized 16-electron isomeric form 2^{R}*. The species with a *fac*-κ^3-*N,C,P* can isomerize to 2^{R}* and is then susceptible to attack by CO.

Density functional theory (DFT) calculations revealed that the energy difference between the two isomeric forms is much greater for the $LutP^{R}$ complexes (Figure 5). For example, 2^{Me} is 13.1 kcal/mol more stable than 2^{Me}* whereas 2^{H} is only 4.8 kcal/mol more stable than 2^{H}*. In part, this explains the greater ease with which we were able to isolate the $LutP^{R}$ complexes. It is noteworthy that the relative stability of 2^{H} over 2^{H}* was highly functionally dependent, potentially because of the rather long Mn−$C_{methine}$ bond. Of the four functionals tested (see the Supporting Information), M06/ma-def2-TZVPP accurately corroborated our experimental observations of 2^{H} as the stable isomer. For 2^{H} only, other basis set and

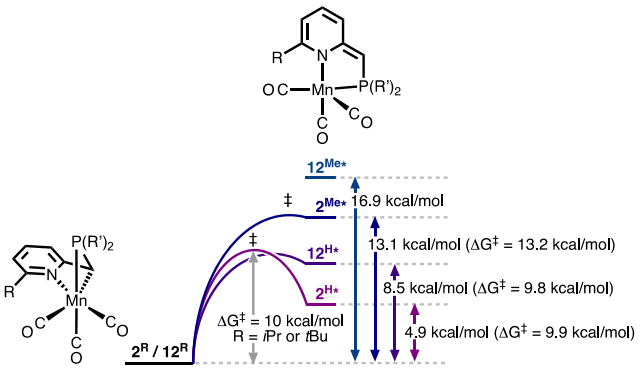

Figure 5. Reaction coordinate diagram with calculated energies for 2^{R} (or 12^{R}) isomerizing into its 16-electron isomer 2^{H}* (or 12^{H}*). Functional: M06. Basis set: ma-def2-TZVPP. 12^{R} is the *i*Pr phosphine-substituted analogue of 2^{R}. The transition state for the step from 12^{Me} to 12^{Me}* was not computed.

functional combinations sometimes gave near-thermoneutral differences between the two isomers (2^{H} vs 2^{H}*); however, for all other complexes, the κ^3-*N,C,P* binding mode was always predicted as the ground state (Figure 5), and hence, we used M06/ma-def2-TZVPP for all further calculations.

DFT calculations predicted exergonic formation of dearomatized tetracarbonyl complexes (3^{R}) relative to 2^{R}, consistent with our observations. We wondered if, although not observed, 2^{R}* was a relevant intermediate in the transformation of 2^{R} into 3^{R} and explored the isomerization using DFT and found that the barrier for converting atypical κ^3-*N,C,P* species 2^{H} into the dearomatized 16-electron isomer 2^{H}* is 9.9 kcal/mol (Figure 5); the *i*Pr analogue had a barrier of 9.8 kcal/mol. This barrier is low enough that a rapid isomerization could occur prior to addition of CO to form 3^{H} [or H_2 activation to form 4^{H} (*vide infra*)]. The barrier for converting atypical κ^3-*N,C,P* species 2^{Me} into the dearomatized 16-electron isomer 2^{Me}* is 13.2 kcal/mol (Figure 5), so it is expected that 2^{Me}* is highly unstable and consistent with our obsrvation that 2^{Me} reacts sluggishly with CO.

Reactivity of κ^3-*N,C,P* Mn(I) Complexes with Reductants. Treatment of a degassed solution of 2^{R} in either C_6D_6 or C_7D_8 with H_2 (1 atm, room temperature) quantitatively afforded the monohydride complexes 4^{R} (Scheme 5). Hydrogen addition was found to be irreversible; for instance, 4^{R} was

Scheme 5. Synthetic Routes to 4^{R}: H_2 Activation across Mn−C Bonds

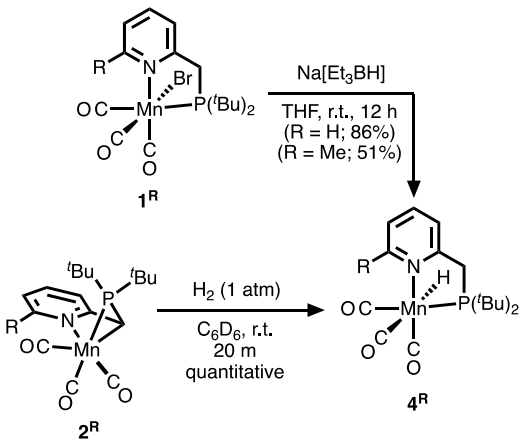

https://doi.org/10.1021/acs.organomet.1c00606
Organometallics 2022, 41, 67−75

unreactive in static vacuum and heat (60 °C). Additionally, 4^{H} was similarly accessed from 3^{H}, albeit requiring several days to reach completion and including observation of some free ligand (Figure S42). The sluggishness of the addition of H_2 to 3^{H} indicates to us that addition of H_2 requires dissociation of CO leading to formation of 2^{H} or its 16-electron isomer 2^{R}* as an intermediate.

The hydride complexes 4^{R} were also accessed directly by treatment of 1^{R} with equimolar Na[Et_3BH] in THF at room temperature (Scheme 5). Both 4^{H} and 4^{Me} exhibit hydride resonances in the ^{1}H NMR spectrum at δ_H −4.17 (d, $^2J_{HP}$ = 53 Hz) and δ_H −4.37 (d, $^2J_{HP}$ = 54 Hz), indicative of a *cis* orientation relative to the tBu_2P group and consistent with FTIR-ATR and XRD data (Figure 6).

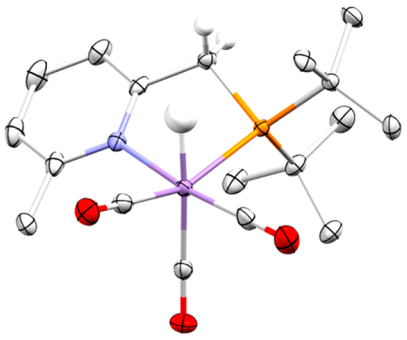

Figure 6. X-ray crystallographically determined molecular structure of 4^{Me} with thermal ellipsoids set at 50% probability. The structure of 4^{H} was not determined. Except for hydride and methylene CH, hydrogen atoms have been omitted for the sake of clarity. Selected bond distances (angstroms): Mn−N, 2.158(2); Mn···$C_{methylene}$, 3.139(3); Mn−P, 2.2958(8).

Treatment of 1^{R} with excess $NaBH_4$ in a toluene/ethanol solvent (4:1) at room temperature led to divergent products. For instance, the product using 1^{Me} results in the formation of *cis*-Mn(LutP)(μ_2,η^1:η^1-H_2BH_2)(CO)$_2$ (5^{Me}) as the major product and 4^{Me} as a concomitantly formed minor byproduct (Scheme 6). However, identical conditions using 1^{H} afford 4^{H} as the major product and a minor component tentatively assigned as 5^{H} that was not isolated.

Scheme 6. Preparation of 5^{Me}

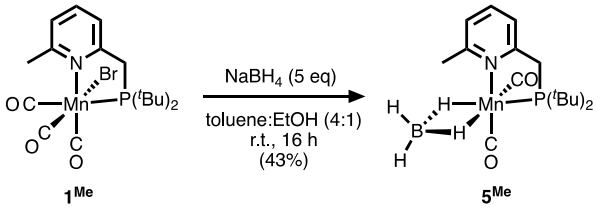

The X-ray structure of 5^{Me} (Figure 7) revealed a Mn(I)-(μ_2,η^1:η^1-H_2BH_2) moiety; despite having been calculated as a favored interaction relative to μ-mono-HBH_3 ligation,[10] this binding mode is relatively rare.[11,12] When 5^{Me} was treated with L-type ligands (e.g., Et_3N or CO), conversion to 4^{Me} was observed along with free ligand and other unidentified decomposition products. Similarly, hydride abstraction using [CPh_3][PF_6] or CO liberation with trimethylamine *N*-oxide resulted in the formation of 4^{Me} and other decomposition products.

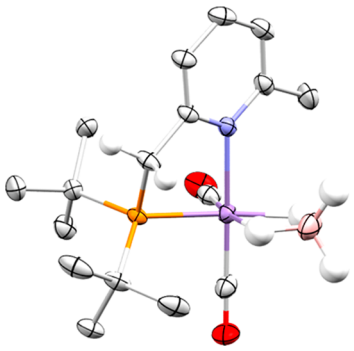

Figure 7. X-ray crystallographically determined molecular structure of 5^{Me} with thermal ellipsoids set at 50% probability. Except for those attached to boron and the methylene carbon, hydrogen atoms have been omitted for the sake of clarity. Selected bond distances (angstroms): Mn−N, 2.140(1); Mn···$C_{methylene}$, 3.098(2); Mn−P, 2.2686(6); Mn···B, 2.157(2).

Reactivity of κ^3-*N,C,P* Mn(I) Complexes with Michael Acceptors and Donors. Activation of organic substrates by the dearomatized pincer compound Mn(PNP^{tBu})(CO)$_2$ was explored by Milstein and co-workers, and the complexes were competent in catalyzed Michael addition of alkyl and aryl nitriles to classical Michael acceptors.[8] Mn(PNP^{tBu})(CO)$_2$ was observed to form a tetradentate complex upon treatment with benzyl cyanide (the Michael donor) to form a templated complex that was implicated as a key intermediate in this transformation. We envisioned that, while Mn(PNP^{tBu})(CO)$_2$ exhibits a dearomatized backbone, similar chemistry might be achieved on our PN system 2^{R} that contains the atypical κ^3-*N,C,P* mode instead. To test this hypothesis, we reacted 2^{Me} with benzyl cyanide, and it too formed a scorpionate complex **6** (Figure 8), which is structurally analogous to the templated complex reported by Milstein.[8] Additionally, an equimolar NMR solution of 2^{Me} and *E*-chalcone in C_6D_6 generated a new species **7** that was characterized by NMR spectroscopy and XRD as a complementary, templated Michael acceptor complex (Scheme 7).

Complex 1^{Me} with a catalytic base (e.g., 10 mol % KO*t*Bu) or 2^{Me} alone was observed to catalyze the Michael addition of benzyl cyanide to methyl acrylate or *E*-chalcone. A control experiment between the same donor and acceptor without the Mn complex and only base showed yields comparable to that of the reaction including 1^{Me} and a base. Although unsurprising,[13] this control reaction calls into question the role of MLC-type catalysts in Michael addition chemistry and hence was not pursued further.

Reactivity of κ^3-*N,C,P* Mn(I) Complexes with $AlCl_3$. In addition to the aforementioned organic substrates, it was observed that the treatment of 2^{R} with $AlCl_3$ resulted in the rapid formation of the facially coordinated, chlorido-bridged complexes, 8^{R} (Scheme 8). These complexes feature a rare Mn-(μ-Cl)-Al motif that, to the best of our knowledge, is the first of its kind with two closely related examples (Figure 9).[14] The Al atom is bonded to the methylene arm, firmly demonstrating the nucleophilicity of the 18-electron complexes containing the κ^3-*N,C,P* mode.

Reactivity of κ^3-*N,C,P* Mn(I) Complexes with Water. The complexes 2^{R} are remarkably sensitive to moisture. In our initial pursuit of these deprotonated complexes, it was observed that if water was not rigorously excluded (passing solvents over a plug of alumina immediately prior to use, for

https://doi.org/10.1021/acs.organomet.1c00606
Organometallics 2022, 41, 67−75

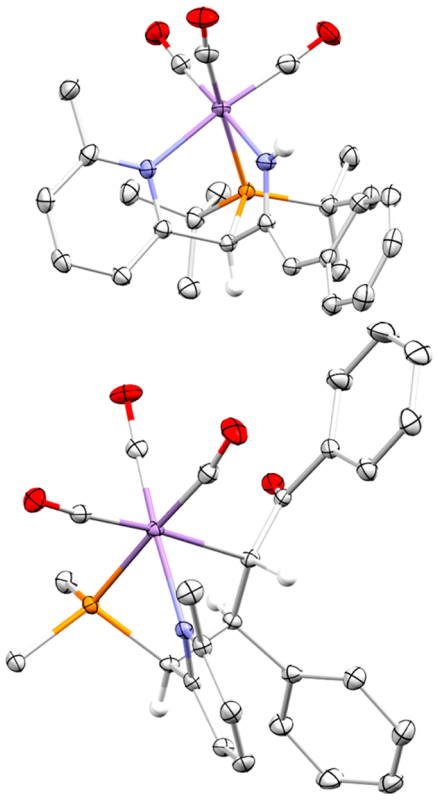

Figure 8. X-ray crystallographically determined molecular structure of **6** (top) and **7** (bottom) with thermal ellipsoids set at 50% probability. Except for NH and methylene CH, hydrogen atoms have been omitted for the sake of clarity. The *t*Bu Me groups for **7** have been removed for the sake of clarity. Selected bond distances (angstroms) for **6**: Mn−N_{py}, 2.138(1); Mn−N_{imine}, 2.030(1); Mn−P, 2.3530(4). Selected bond distances (angstroms) for **7**: Mn−N, 2.123(1); Mn−$C_{chalcone}$, 2.256(1); Mn−P, 2.3556(4).

Scheme 7. Preparation of 6 and 7

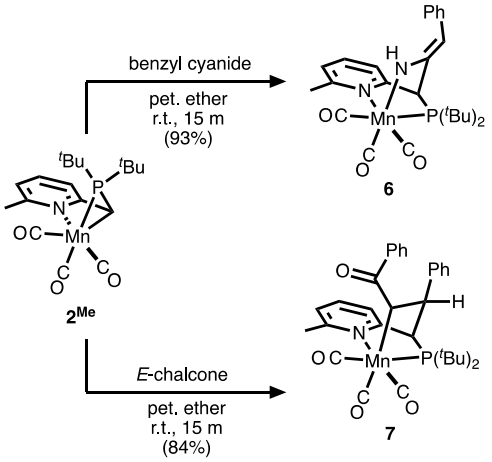

instance), metallocarboxylate complexes 9^R were obtained instead of 2^R. In fact, 9^R was discovered from the reaction of 2^R with adventitious water in a glovebox. Independent synthesis was accomplished by treating 2^H with 2 equiv of water in dry benzene (Scheme 9). A rapid change in color was observed, and 9^H subsequently precipitated. These metallocarboxylate complexes are dark red in color and exhibit seven carbonyl stretches in their FTIR-ATR spectra. Additionally, they have poor solubility and/or stability in common organic solvents,

Scheme 8. Preparation of 8^H

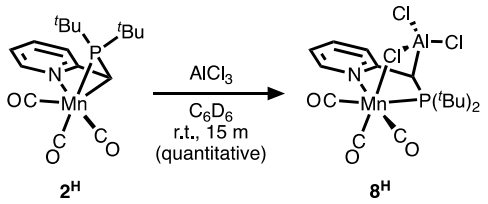

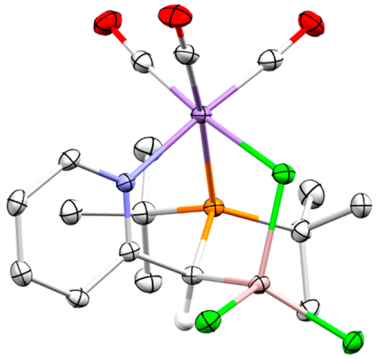

Figure 9. X-ray crystallographically determined molecular structure of 8^H with thermal ellipsoids set at 50% probability. Except for methine CH, hydrogen atoms have been omitted for the sake of clarity. Selected bond lengths (angstroms): Mn−N, 2.074(1); Mn−Cl, 2.4846(4); Mn−P, 2.3907(4); Al−C, 2.019(1).

Scheme 9. Preparation of 9^R

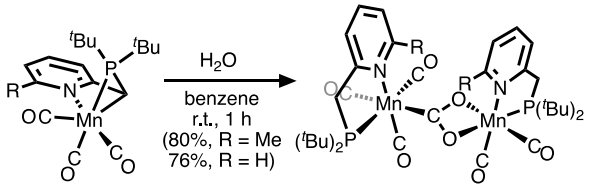

precluding their complete characterization by NMR spectroscopy. However, isolated crystalline 9^R from hydrated solutions of 2^R allowed for X-ray quality crystals that confirmed our structural assignments (Figure 10). To the best of our knowledge, 9^R is the first example of a "class I homobimetallic $[Mn(I)]_2(\mu_2\text{-}\eta^3\text{-}CO_2)$" complex[15] and may be somewhat relevant in the chemistry of Mn(I)-catalyzed CO_2 reduction and CO oxidation.[16]

The formation of 9^R likely occurs by initial protonation of 2^R to generate a hydroxide ion that attacks a coordinated CO ligand forming a metallocarboxylic acid intermediate; this mechanism has been proposed to be operative in the oxidation of CO.[17] The metallocarboxylic acid in turn protonates another equivalent of 2^R, resulting in the observed metallocarboxylate moiety in 9^R.

Treatment of 1^R with Alkoxide Bases. Dehydrohalogenation of 1^R with alkoxide bases, as opposed to $K[N(SiMe_3)_2]$, resulted in varying outcomes across the two ligands. For instance, dehydrohalogenation of 1^{Me} with KO*t*Bu afforded 2^{Me} as the major product. In contrast, treatment of 1^H with KO*t*Bu does not afford 2^H and instead affords a tentatively assigned alkoxide complex $[\{PicP\}Mn(CO)_3OtBu]$ (10^H) (δ_P 136), 3^H, and a free ligand (Scheme 10 and Figure S75−S78).

Our assignment for 10^H is based on the following set of experiments and observations. First, the ^1H NMR spectrum of

https://doi.org/10.1021/acs.organomet.1c00606
Organometallics 2022, 41, 67−75

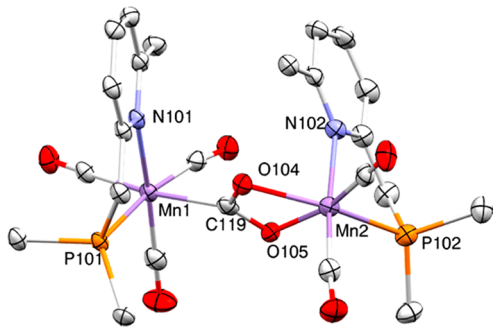

Figure 10. X-ray crystallographically determined molecular structure of one of the molecules found within the unit cell of $\mathbf{9^{Me}}$ with thermal ellipsoids set at 50% probability. Hydrogen atoms and disordered solvent molecules have been omitted for the sake of clarity. The *t*Bu Me groups have been omitted for the sake of clarity. A partial structure of $\mathbf{9^{H}}$ was collected to confirm identical connectivity. Selected bond lengths (angstroms): Mn1−N101, 2.167(2); Mn1−P101, 2.3500(7); Mn1−C119, 2.061(3); Mn2−N102, 2.168(2); Mn2−P102, 2.2681(9); Mn2−O104, 2.077(2); Mn2−O105, 2.062(2).

Scheme 10. Alkoxide Complex Formation

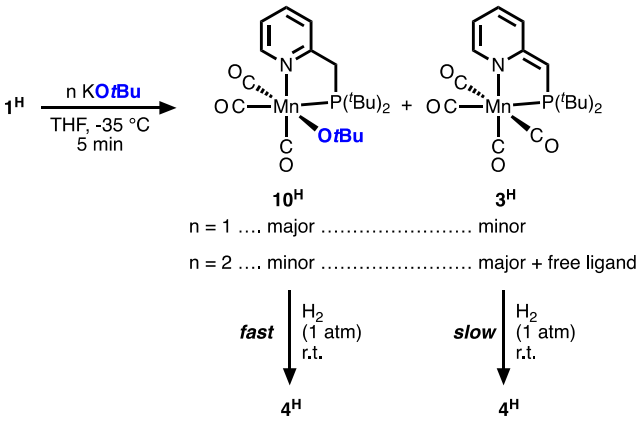

$\mathbf{10^{H}}$ indicates that the PicP ligand is aromatized (Figure S75). Second, independently prepared $\mathbf{2^{H}}$ converts into $\mathbf{10^{H}}$ upon being treated with dry *t*BuOH (1 equiv) (Figure S81). Third, treatment of a mixture of $\mathbf{10^{H}}$ and $\mathbf{3^{H}}$ with H_2 affords $\mathbf{4^{H}}$ (Figure S82). Note that this reaction resulted in rapid consumption of $\mathbf{10^{H}}$ relative to the slow consumption of $\mathbf{3^{H}}$, both of which form $\mathbf{4^{H}}$ (Scheme 10). We also treated $\mathbf{1^{H}}$ with NaO*i*Pr and obtained a compound with similarly positioned ^{31}P and ^{1}H NMR signals (Figures S79 and S80). $\mathbf{10^{H}}$ is exceedingly sensitive to moisture, usually forming $\mathbf{9^{H}}$, and as a result, the isolation of $\mathbf{10^{H}}$ was not accomplished in this study.

Catalytic Alkene Hydrogenation and Coordination Chemistry of Isopropyl-Substituted Complexes. While this work was being prepared, Khusnutdinova demonstrated that the *i*Pr-phosphine analogue of $\mathbf{1^{H}}$ ($\mathbf{11^{H}}$) was an alkene hydrogenation catalyst.[7] Therefore, we synthesized $\mathbf{11^{H}}$ and its Lut$\mathrm{P}^{i\mathrm{Pr}}$ analogue $\mathbf{11^{Me}}$ and compared their catalytic activity to that of $\mathbf{1^{R}}$. All four complexes, $\mathbf{1^{Me}}$, $\mathbf{1^{H}}$, $\mathbf{11^{Me}}$, and $\mathbf{11^{H}}$, performed effectively identically in catalytic styrene hydrogenation to ethylbenzene (88 ± 3% isolated yield) (Scheme 11); it should be noted that special care was required to ensure that the catalytic setup was not exposed to moisture, except for the chemistry associated with $\mathbf{11^{H}}$ that appears to be slightly more robust than the other systems.

Scheme 11. Catalytic Styrene Hydrogenation[18]

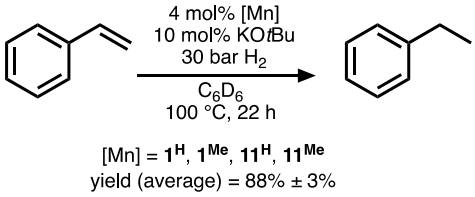

Unsurprisingly, the chemistries of $\mathbf{11^{R}}$ and $\mathbf{1^{R}}$ are analogous, and accordingly, when $\mathbf{11^{Me}}$ was dehydrohalogenated with K[N(SiMe$_3$)$_2$], the κ^3-*N,C,P* complex $\mathbf{12^{Me}}$ was the sole product and was fully characterized (Figure 11). Much like $\mathbf{2^{Me}}$, $\mathbf{12^{Me}}$ was relatively stable under dry conditions and did not convert into a tetracarbonyl species when heated or treated with CO.[19]

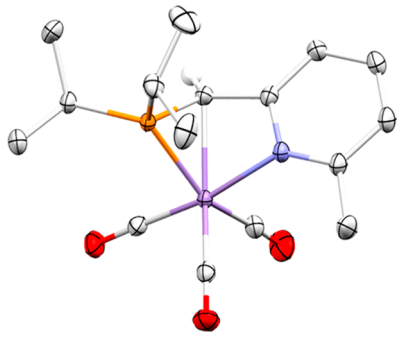

Figure 11. X-ray crystallographically determined molecular structure of one of the molecules found within the unit cell of $\mathbf{12^{Me}}$ with thermal ellipsoids set at 50% probability. Except for the methine CH proton, hydrogen atoms have been omitted for the sake of clarity. Selected bond lengths (angstroms): Mn−N, 2.079(1); Mn−C, 2.185(2); Mn−P, 2.2304(5).

The solutions containing species derived from $\mathbf{11^{H}}$ were complicated and difficult to interpret, and we failed in attempts to isolate them, consistent with what others have observed.[7] The coordination chemistry we uncovered with the other complexes greatly aided our ability to interpret the complicated speciation associated with dehydrohalogenation of $\mathbf{11^{H}}$ (Scheme 12).

For example, dehydrohalogenation of $\mathbf{11^{H}}$ with K[N(SiMe$_3$)$_2$] resulted in the formation of a multitude of species (Figure S95). One is tentatively assigned as the κ^3-*N,C,P* complex ($\mathbf{12^{H}}$) on the basis of its ^{1}H and ^{31}P{^{1}H} NMR spectral similarities with $\mathbf{12^{Me}}$ (Figures S94 and S95). Another species has a broad ^{31}P{^{1}H} NMR resonance at δ_P 80 and has chemical behavior similar to that of the dearomatized tetracarbonyl $\mathbf{3^{H}}$. For instance, the intensity of this feature at δ_P 80 continues to increase as solutions containing $\mathbf{12^{H}}$ are heated and is accompanied by formation of a free ligand. Finally, another unidentified species with a sharp ^{31}P{^{1}H} NMR resonance at δ_P 91 is apparent upon initial dehydrohalogenation but quickly disappears over the course of 24 h. As noted, the complicated nature of the mixture inhibited further interpretation.

Mechanistic Considerations and Implications of the κ^3-*N,C,P* Binding Mode. Some possible mechanisms of the alkene hydrogenation were considered. In one extreme, the mechanism is outer sphere in nature as proposed by others.[7] At

https://doi.org/10.1021/acs.organomet.1c00606
Organometallics 2022, 41, 67−75

Scheme 12. Summary of Coordination Chemistry Using *i*Pr-Substituted PicP and LutP

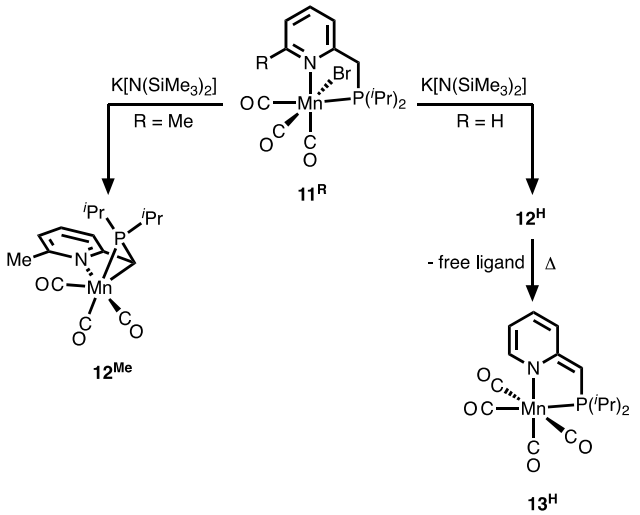

the other extreme, an inner sphere process occurs, where a Mn(I)-ethylbenzene species forms as a key intermediate.[20] From such an intermediate, a likely reaction is σ-CAM between H_2 and Mn(I)-ethylbenzene.[20,21] Another likely possibility is a radical pathway to form a Mn(I)-ethylbenzene intermediate that is further attacked by another Mn-H species, analogous to the radical mechanism empirically demonstrated by Baird and Halpern.[22]

We found that the bromido amino-phosphine precatalyst to **A** (Scheme 1) catalyzed styrene hydrogenation (53%), and control experiments with $Mn(CO)_5Br$ and a base were also catalytically active (20%).[7] Given that these and other comparable Mn(I) catalysts are free of additives or use a substoichiometric base, it seems unlikely that atypical or even typical MLC is involved in catalytic cycles. Rather, radical mechanisms are plausible given their known involvement in Mn(I)-H-mediated alkene hydrogenation[22] and the prevalence of radical paths in first-row metal-catalyzed reactions.

CONCLUSION

Dehydrohalogenation of the picolinyl- and lutidinyl-derived PN-Mn(I) complexes afforded 18-electron aromatized complexes with a κ^3-*N,C,P* binding mode. This binding mode is atypical, and hitherto unexpected, of the traditional 16-electron isomeric dearomatized form in the A/D-MLC paradigm. In contrast to traditional A/D-MLC systems, the reactive κ^3-*N,C,P* complexes activate dihydrogen across a bonded Mn−C moiety to afford hydride complexes, although we cannot rule out activation on a dearomatized system because a low barrier (≈10 kcal/mol) for isomerization was computed with DFT.

The nucleophilicity of the κ^3-*N,C,P* binding mode was demonstrated through reactions with a variety of electrophiles. Of particular note is the formation of adducts with Michael acceptors and donors. $\mathbf{1}^{\mathbf{R}}$ was effective in catalytic Michael addition reactions, akin to its PNP^{tBu} analogue, but control reactions with just a base {e.g., KO*t*Bu or $K[N(SiMe_3)_2]$} are unsurprisingly also effective. This calls into question the importance of these and related Mn compounds in catalyzed Michael additions. We also used $\mathbf{1}^{\mathbf{R}}$ and $\mathbf{11}^{\mathbf{R}}$ in catalytic styrene hydrogenation and found that all four complexes are essentially the same, performing better than simple systems like $Mn(CO)_5Br$ with a base or its amino-phosphine analogue (**A**). Collectively, these findings promote the idea that, while tempting, A/D-MLC steps may not be important in catalytic transformations. Nonetheless, the novel coordination modes and reactivity of the atypical binding mode should be considered a viable starting point in catalyst activation reactions.

ASSOCIATED CONTENT

Supporting Information

The Supporting Information is available free of charge at https://pubs.acs.org/doi/10.1021/acs.organomet.1c00606.

Procedures and characterization data for novel compounds (PDF)

Additional structural data (XYZ)

Accession Codes

CCDC 2115073−2115083 contain the supplementary crystallographic data for this paper. These data can be obtained free of charge via www.ccdc.cam.ac.uk/data_request/cif, or by emailing data_request@ccdc.cam.ac.uk, or by contacting The Cambridge Crystallographic Data Centre, 12 Union Road, Cambridge CB2 1EZ, UK; fax: +44 1223 336033.

AUTHOR INFORMATION

Corresponding Author

David C. Lacy − *Department of Chemistry, University at Buffalo, State University of New York, Buffalo, New York 14260, United States;* orcid.org/0000-0001-5546-5081; Email: dclacy@buffalo.edu

Authors

Vipulan Vigneswaran − *Department of Chemistry, University at Buffalo, State University of New York, Buffalo, New York 14260, United States;* orcid.org/0000-0002-8780-8592

Preshit C. Abhyankar − *Department of Chemistry, University at Buffalo, State University of New York, Buffalo, New York 14260, United States;* orcid.org/0000-0002-2283-7122

Samantha N. MacMillan − *Department of Chemistry & Chemical Biology, Cornell University, Ithaca, New York 14853, United States;* orcid.org/0000-0001-6516-1823

Complete contact information is available at: https://pubs.acs.org/10.1021/acs.organomet.1c00606

Notes

The authors declare no competing financial interest.

ACKNOWLEDGMENTS

The authors acknowledge the University at Buffalo (UB) and National Science Foundation Grant 1847933 for funding. Computations were completed at the UB Center for Computational Research, and FT-ICR data (S10 RR029517) were collected at the UB Chemistry Instrument Center (CIC). Professor Jochen Autschbach is acknowledged for advice with DFT calculations.

REFERENCES

(1) Selected recent reviews: (a) Wang, Y.; Wang, M.; Li, Y.; Liu, Q. Homogeneous manganese-catalyzed hydrogenation and dehydrogenation reactions. *Chem.* **2021**, *7*, 1180−1223. (b) Azouzi, K.; Valyaev, D. A.; Bastin, S.; Sortais, J.-B. Manganese − New prominent actor in transfer hydrogenation catalysis. *Current Opinion in Green Sustainable Chemistry* **2021**, *31*, 100511. (c) Zell, T.; Langer, R. From ruthenium to iron and manganese—a mechanistic view on challenges and design

principles of base-metal hydrogenation catalysts. *ChemCatChem* **2018**, *10*, 1930.
(2) Agbossou-Niedercorn, F.; Michon, C. Bifunctional homogeneous catalysts based on first row transition metals in asymmetric hydrogenation. *Coord. Chem. Rev.* **2020**, *425*, 213523.
(3) Elsby, M. R.; Baker, R. T. Strategies and mechanisms of metal-ligand cooperativity in first-row transition metal complex catalysts. *Chem. Soc. Rev.* **2020**, *49*, 8933−8987.
(4) (a) Dub, P. A.; Gordon, J. C. The role of the metal-bound N-H functionality in Noyori-type molecular catalysts. *Nat. Rev. Chem.* **2018**, *2*, 396−408. (b) Dub, P. A.; Gordon, J. C. The mechanism of enantioselective ketone reduction with Noyori and Noyori−Ikariya bifunctional catalysts. *Dalton Trans.* **2016**, *45*, 6756−6781.
(5) (a) Goncalves, T. P.; Dutta, I.; Huang, K. Aromaticity in catalysis: metal ligand cooperation via ligand dearomatization and rearomatization. *Chem. Commun.* **2021**, *57*, 3070. (b) Shimbayashi, T.; Fujita, K. Recent advances in homogeneous catalysis via metal-ligand cooperation involving aromatization and dearomatization. *Catalysts* **2020**, *10*, 635.
(6) Vigneswaran, V.; MacMillan, S. N.; Lacy, D. C. *β*-amino phosphine Mn catalysts for 1,4-transfer hydrogenation of chalcones and allylic alcohol isomerization. *Organometallics* **2019**, *38*, 4387−4391.
(7) Rahaman, S. M. W.; Pandey, D. K.; Rivada-Wheelaghan, O.; Dubey, A.; Fayzullin, R. R.; Khusnutdinova, J. R. Hydrogenation of alkenes catalyzed by a non-pincer Mn complex. *ChemCatChem* **2020**, *12*, 5912−5918.
(8) Nerush, A.; Vogt, M.; Gellrich, U.; Leitus, G.; Ben-David, Y.; Milstein, D. Template catalysis by metal-ligand cooperation. C-C bond formation via conjugate addition of non-activated nitriles under mild, base-free conditions catalyzed by a manganese pincer complex. *J. Am. Chem. Soc.* **2016**, *138*, 6985−6997.
(9) (a) Kireev, N. V.; Filippov, O. A.; Gulyaeva, E. S.; Shubina, E. S.; Vendier, L.; Canac, Y.; Sortais, J.-B.; Lugan, N.; Valyaev, D. A. Bis[diphenylphosphino]methane and ist bridge-substituted analogues as chemically non-innocent ligands for H_2 activation. *Chem. Commun.* **2020**, *56*, 2139−2142. (b) Buhaibeh, R.; Filippov, O. A.; Bruneau-Voisine, A.; Willot, J.; Duhayon, C.; Valyaev, D. A.; Lugan, N.; Canac, Y.; Sortais, J.-B. Phosphine-NHC manganese hydrogenation catalyst exhibiting a non-classical metal-ligand cooperative H_2 activation mode. *Angew. Chem., Int. Ed.* **2019**, *58*, 6727−6731. (c) Chakraborty, S.; Gellrich, R.; Diskin-Posner, Y.; Leitus, G.; Avram, L.; Milstein, D. Manganese-catalyzed N-formylation of amines by methanol liberating H_2: a catalytic and mechanistic study. *Angew. Chem., Int. Ed.* **2017**, *56*, 4229−4233.
(10) Oishi, Y.; Albright, A. T.; Fujimoto, H. Fluxionality in $(BH_4)Mn(CO)_4$ and $(BH_4)Cu(PH_3)_2$. *Polyhedron* **1995**, *14*, 2603−2612.
(11) (a) Agnew, D. W.; Moore, C. E.; Rheingold, A. L.; Figueroa, J. S. Controlled cis labilization of CO from manganese(I) mixed carbonyl/isocyanide complexes: an entry point to coordinatively unsaturated metallo-Lewis acids. *Organometallics* **2017**, *36*, 363−371. (b) Price, J. S.; DeJordy, D. M.; Emslie, D. J. H.; Britten, J. F. Reactions of $[(dmpe)_2MnH(C_2H_4)]$: synthesis and characterization of manganese(I) borohydride and hydride complexes. *Dalton Trans.* **2020**, *49*, 9983−9994.
(12) Merle, N.; Frost, C. G.; Kociok-Köhn, G.; Willis, M. C.; Weller, A. S. Chelating phosphane-boranes as hemilabile ligands − synthesis of $[Mn(CO)_3(\eta^2\text{-}H_3B{\cdot}dppm)][BArF_4]$ and $[Mn(CO)_4(\eta^1\text{-}H_3B{\cdot}dppm)][BArF_4]$. *Eur. J. Inorg. Chem.* **2006**, *2006*, 4068−4073.
(13) Sai, M.; Kurouchi, H. Potassium base-catalyzed Michael additions of allylic alcohols to *α,β*-unsaturated amides: scope and mechanistic insights. *Adv. Synth. Catal.* **2021**, *363*, 3585−3591.
(14) (a) Butts, S. B.; Strauss, S. H.; Holt, E. M.; Stimson, R. E.; Alcock, N. W.; Shriver, D. F. Activation of coordinated carbon monoxide toward alkyl and aryl migration (carbon monoxide insertion) by molecular Lewis acids and x-ray structure of the reactive intermediate. *J. Am. Chem. Soc.* **1980**, *102*, 5093−5100. (b) Richmond, T. G.; Basolo, F.; Shriver, D. F. Bifunctional activation of coordinated carbon monoxide: a kinetic study of Lewis acid induced alkyl migration. *Inorg. Chem.* **1982**, *21*, 1272−1273.
(15) Gibson, D. H. The organometallic chemistry of carbon dioxide. *Chem. Rev.* **1996**, *96*, 2063−2095.
(16) Sinopoli, A.; La Porte, N. T.; Martinez, J. F.; Wasielewski, M. R.; Sohail, M. Manganese carbonyl complexes for CO_2 reduction. *Coord. Chem. Rev.* **2018**, *365*, 60−74.
(17) (a) Harkness, A. C.; Halpern, J. Oxidation of carbon monoxide by metal ions. *J. Am. Chem. Soc.* **1961**, *83*, 1258−1259. (b) Grice, N.; Kao, S. C.; Pettit, R. Chemical properties of metallocarboxylic acids of transition metals. *J. Am. Chem. Soc.* **1979**, *101*, 1627−1628.
(18) Actual yields likely quantitative. Some ethylbenzene is lost during venting the Parr reactor. No styrene was observed at the end of catalysis.
(19) Extended reaction with CO (>4 days) results in decomposition to unidentified compounds.
(20) Weber, S.; Stöger, B.; Veiros, L. F.; Kirchner, K. Rethinking basic concepts−hydrogenation of alkenes catalyzed by bench-stable alkyl Mn(I) complexes. *ACS Catal.* **2019**, *9*, 9715−9720.
(21) Perutz, R. N.; Sabo-Etienne, S. The sigma-CAM mechanism: sigma complexes as the basis of sigma bond metathesis at late-transition-metal centers. *Angew. Chem., Int. Ed.* **2007**, *46*, 2578−2592.
(22) (a) Wassink, B.; Thomas, M. J.; Wright, S. C.; Gillis, J. J.; Baird, M. C. Mechanisms of the hydrometallation ("insertion") and stoichiometric hydrogenation reactions of conjugated dienes effected by manganese pentacarbonyl hydride: process involving the radical pair mechanism. *J. Am. Chem. Soc.* **1987**, *109*, 1995−2002. (b) Sweany, R. L.; Halpern, J. Hydrogenation of alpha-methylstyrene by hydridopentacarbonylmanganese (I). Evidence for a free-radical mechanism. *J. Am. Chem. Soc.* **1977**, *99*, 8335−8337.

https://doi.org/10.1021/acs.organomet.1c00606
Organometallics 2022, 41, 67−75